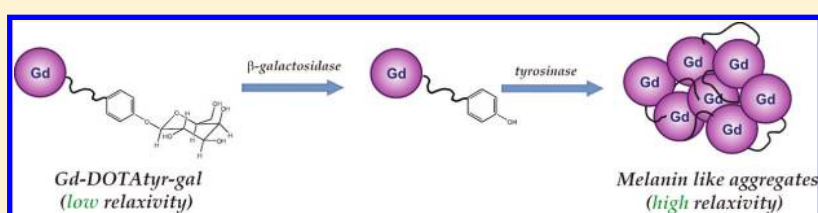


## $\beta$ -Gal Gene Expression MRI Reporter in Melanoma Tumor Cells. Design, Synthesis, and *in Vitro* and *in Vivo* Testing of a Gd(III) Containing Probe Forming a High Relaxivity, Melanin-Like Structure upon $\beta$ -Gal Enzymatic Activation

Francesca Arena, Jebasingh Bhagavath Singh, Eliana Gianolio, Rachele Stefania, and Silvio Aime\*

Centro di Imaging Molecolare, Dipartimento di Chimica IFM, Università degli Studi di Torino, Via Nizza 52, 10126 Torino, Italy

### S Supporting Information



**ABSTRACT:** The aim of this work is to design and test an MRI probe (Gd-DOTAtyr-gal) able to report on the gene expression of  $\beta$ -galactosidase ( $\beta$ -Gal) in melanoma cells. The probe consists of a Gd-DOTA reporter bearing on its surface a tyrosine-galactose-pyranose functionality that, upon the release of the sugar moiety, readily transforms, in the presence of tyrosinase, into melanin oligomeric/polymeric mixture. The formation of Gd-DOTA-containing melanin oligomers and polymers is accompanied by a marked increase of the water proton relaxation rate. The steps involving the release of the galactose-pyranose group and the formation of the melanin-like structure have been carefully investigated *in vitro* by relaxometric and UV-vis measurements. Cellular uptake studies of Gd-DOTAtyr-gal by melanoma cells have shown that the probe enters the cells, and it appears not to be confined in endosomal vesicles. Using B16-F10LacZ transfected cells, the fast formation of paramagnetic melanin-Gd(III)-containing species has been assessed by the measurement of increased longitudinal relaxation rates of the cellular pellets suspensions. The *in vitro* results have been confirmed in *in vivo* MRI investigations on murine melanoma tumor bearing mice. Upon direct injection of Gd-DOTAtyr-gal, a good contrast is observed after 5 h post injection in B16-F10LacZ tumors, but not in B16-F10 tumors lacking the  $\beta$ -Gal enzyme. Gd-DOTAtyr-gal in combination with tyrosinase introduces a novel approach for the detection of  $\beta$ -Gal expression by MRI *in vivo*.

### INTRODUCTION

The development of reliable means to follow gene expression *in vitro* and *in vivo* has attracted great interest in recent years. Gene expression is commonly monitored by introducing a marker gene to follow the regulation of the gene of interest.<sup>1</sup> The bacterial *LacZ* gene is a very popular gene reporter, with applications ranging from immunosorbent assays to *in situ* hybridizations and evaluation of gene distributions. Indeed, *LacZ* has been used in medical trials revealing regions of tissue transfection in biopsy specimens based on histologic staining. As such, many colorimetric stains and assays have been developed and are in routine use, including reagents such as nitrophenyl- $\beta$ -D-galactopyranoside, which generates a yellow color, or 4-chloro-3-bromoindole-galactose, which gives a blue stain, and 3,4-cyclohexenoesculetin  $\beta$ -D-galactopyranoside, which yields a black stain, respectively.<sup>2</sup> The application of such methods has various drawbacks such as the need for histological processing of the region of interest. Magnetic Resonance Imaging offers an alternative to light microscopy, allowing the investigation of intact tissues at the cellular resolution level. The first attempt to tackle the issue of MRI visualization of  $\beta$ -Gal gene expression was carried out by Meade

and co-workers by reporting that the relaxivity of a galactopyranose-substituted tetraazamacrocycle coordinated to a Gd(III) ion can be specifically “switched on” by removing the sugar with  $\beta$ -galactosidase.<sup>3</sup> Unfortunately, the gain in relaxivity brought about by the activation step is relatively small (for several reasons as elucidated in a successive paper from the same author).<sup>4</sup>

Since Meade’s seminal work, MRI detection of  $\beta$ -Gal expression has been under intense scrutiny with the aim of exploring amplification routes that would allow its improved implementation in *in vivo* studies.

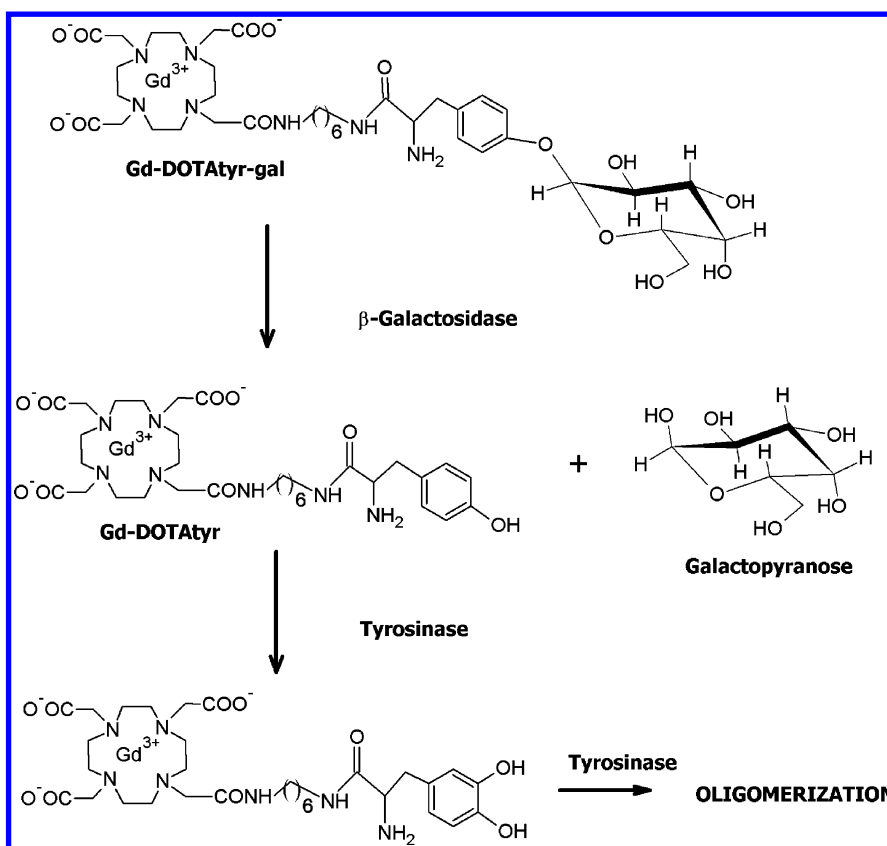
Hanaoka et al. reported on the exploitation of the RIME (receptor-induced magnetization enhancement) by using a  $\beta$ -Gal-activated Gd(III) bearing agent which, upon release of the  $\beta$ -galactopyranoside moiety, enhances its relaxivity thanks to the binding to HSA.<sup>5</sup> A similar attempt to amplify the MRI response of a  $\beta$ -Gal responsive Gd(III) complex has been pursued by Yun-Ming Wang et al.<sup>6</sup>

**Received:** September 8, 2011

**Revised:** October 24, 2011

**Published:** October 31, 2011

Chart 1. Schematic Representation of the Oligomerization Process Achieved upon the Action of  $\beta$ -Galactosidase and Tyrosinase Enzymes



These results represent an interesting proof-of-concept of the RIME approach, but its transaction to cellular and animal applications might be hampered by the fact that  $\beta$ -Gal is in the cytoplasm and HSA is mainly in the extracellular compartments.

As one of the key issues for a successful *in vivo* application deals with the internalization of the probe, Engelmann et al.<sup>7</sup> tackled the problem of penetrating the cell membrane by endowing the surface of a Gd(III) complex with a suitable cationic peptide sequence. The cell-penetrating peptide is bound to a galacto-pyranose moiety and the linkage is selectively cleaved only in  $\beta$ -Gal transfected cells. Thus, the cell accumulation of the MRI agent would be possible only upon  $\beta$ -Gal enzymatic transformation, as the unconverted metal complex could effectively efflux from the cells.

Another efficient method to accumulate a metal complex inside cells relies on the formation of oligo/polymeric structures such as those obtained by Bodganov et al.<sup>8–11</sup> They found that melanin-like macromolecules can form when hydroxo-functionalized Gd(III) chelates are in the presence of tyrosinase or myeloperoxidase.

In the present work, which aims at exploiting the latter route in order to amplify the MRI response at the targeted cells, the designed probe consists of a Gd-DOTA monoamide chelate bearing a tyrosine –OH functionality protected by a galactose moiety (Gd-DOTAtyr-gal). Upon cleavage of the galactose moiety (step activated by the action of  $\beta$ -galactosidase), the tyrosine group, in the Gd-DOTAtyr product, becomes available for the tyrosinase activated melanin polymerization. The formation of the paramagnetic melanin-like macromolecule can be assessed by MRI because the relaxivity of Gd(III)-

complexes increases, in the field range 0.5–1.5 T, if they are part of macromolecular systems, as a consequence of the lengthening of their reorientational correlation time ( $\tau_R$ ) (Chart 1).

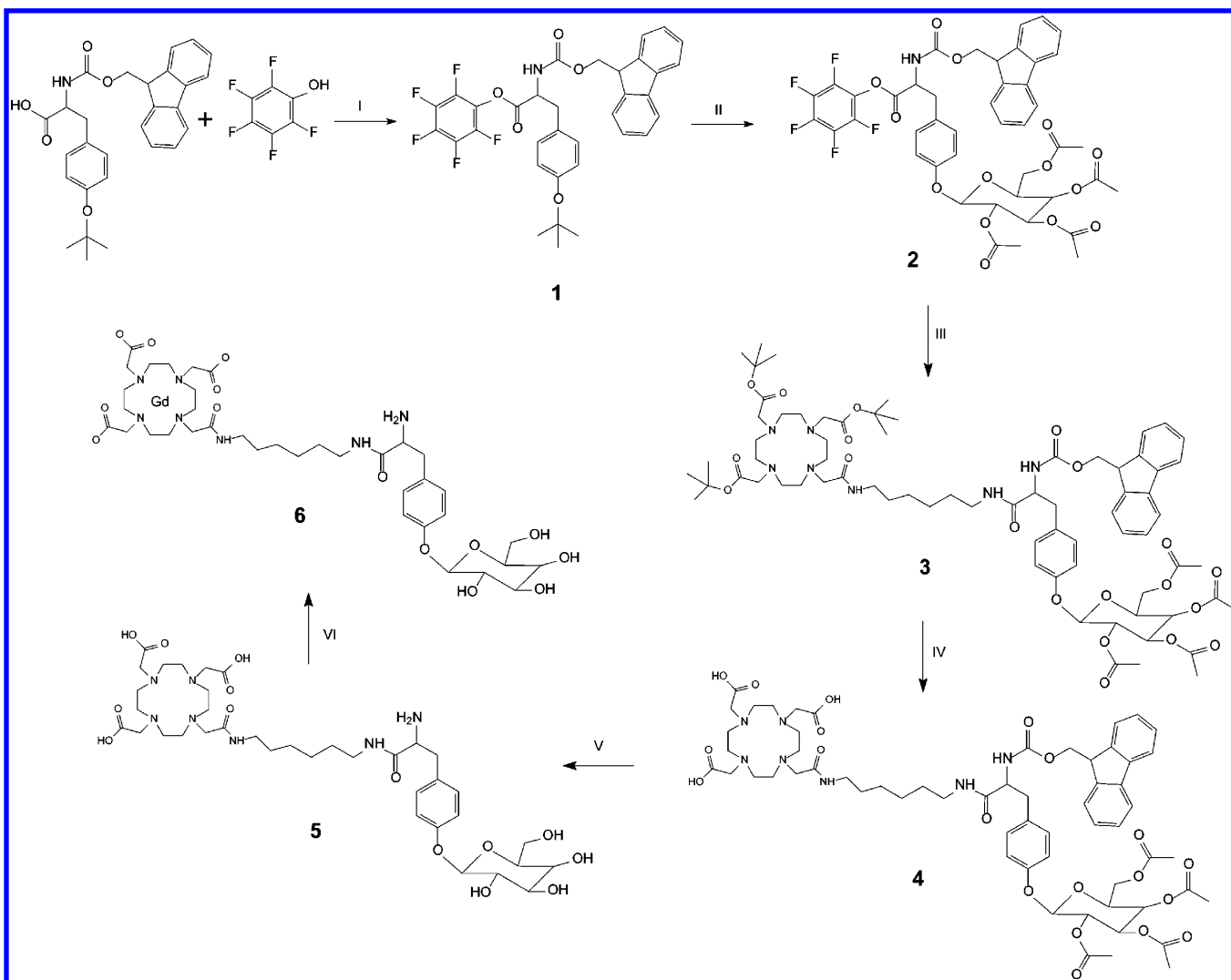
The  $\beta$ -galactosidase-responsive probe has been tested in B16–F10 and B16–F10*LacZ* murine melanoma cells. Melanoma cells have been used for the enzymatic assays, as these cells possess high tyrosinase activity as witnessed by their natural melanin pigmentation. We also demonstrated the ability of Gd-DOTAtyr-gal to visualize stably expressing *LacZ* melanoma tumors *in vivo* upon its direct intratumoral injection.

## EXPERIMENTAL PROCEDURES

**Materials.** All reagents used for the synthesis of DOTAtyr-gal and DOTAtyr ligands were purchased from Sigma Aldrich Co.  $\beta$ -galactosidase (product no. G5635–5KU isolated from *Escherichia coli*) was purchased from Sigma Aldrich and used without any further purification.  $\beta$ -Gal Staining Kit was purchased from Invitrogen. Tyrosinase isolated from *Mushroom* was obtained from Sigma-Aldrich.

NMR spectra were recorded on JEOL Eclipse Plus400 and Bruker Avance 600 spectrometers operating at 9.4 and 14 T, respectively. ESI mass spectra were recorded on a Waters Micromass ZQ Analytical and preparative HPLC-MS were carried out on Waters FractionLynx autopurification system equipped with Waters 2996 diode array and Waters Micromass ZQ (ESCI ionization mode) detectors. DOTAMA-(*tert*-Bu)<sub>3</sub>C<sub>6</sub>NH<sub>2</sub> was prepared following a reported procedure.<sup>12</sup>

**Synthesis of Gd(III) complexes (Scheme 1 and Scheme 2).** *Synthesis of N-(9-Fluorenylmethoxycarbonyl)-O-1,1(dimethyl)ethyl-tyrosine pentafluorophenyl Ester*

Scheme 1. Synthetic Pathway to Gd-DOTATyr-gal<sup>a</sup>

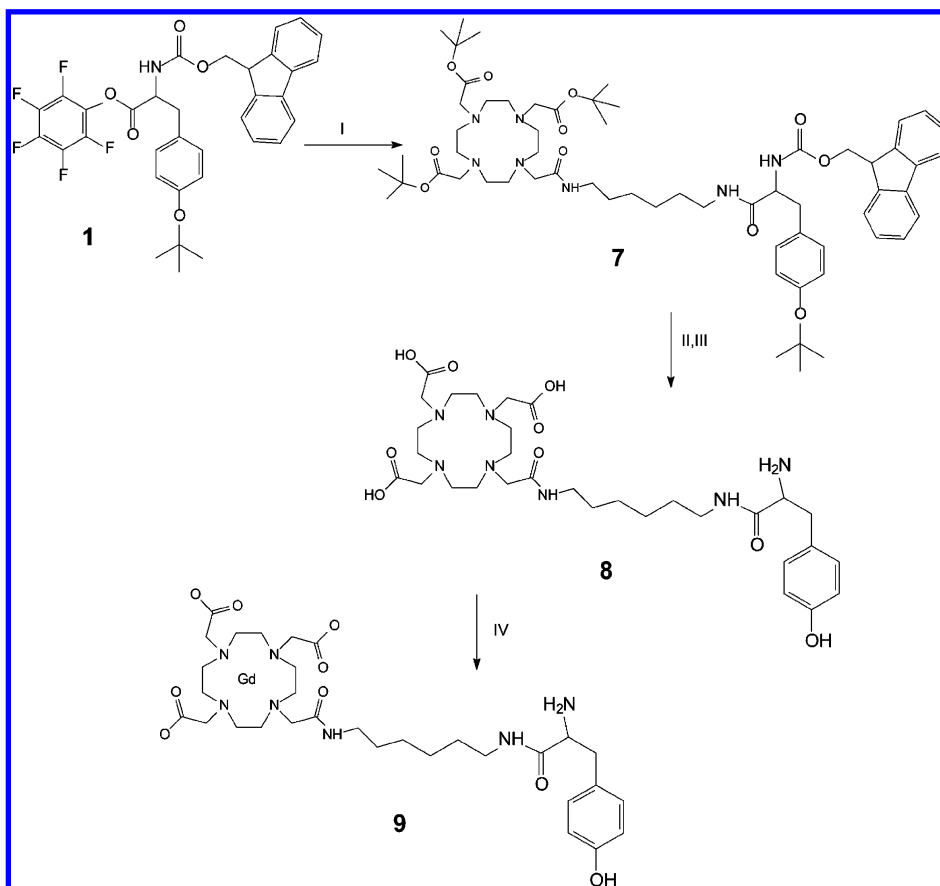
<sup>a</sup>(I) EDCI, CH<sub>2</sub>Cl<sub>2</sub>; (II) Acetobromogalactose, AgOTf, CH<sub>2</sub>Cl<sub>2</sub> dry; (III) DOTAMA(OtBu)<sub>3</sub>C<sub>6</sub>NH<sub>2</sub>, HOBt, CH<sub>2</sub>Cl<sub>2</sub>; (IV) TFA, CH<sub>2</sub>Cl<sub>2</sub>; (V) NaOMe, MeOH; (VI) GdCl<sub>3</sub>, H<sub>2</sub>O, pH 7.

(1). A solution of Fmoc-Tyr-(tBu)OH (2 g, 4.35 mmol), pentafluorophenol (0.8 g, 4.35 mmol) and EDCI (0.834 g, 4.35 mmol) in CH<sub>2</sub>Cl<sub>2</sub> (60 mL) was stirred overnight at 0 °C. The solution was transferred to a separatory funnel and washed with water (2 × 10 mL). The organic layer was dried over anhydrous Na<sub>2</sub>SO<sub>4</sub>, and the solvent was removed under reduced pressure to give the product as a white solid in quantitative yield. <sup>1</sup>H NMR (400 MHz, CDCl<sub>3</sub>): δ 1.33 (s, 9H), 3.21 (m, 2H), 4.21 (t, 1H), 4.43 (m, 2H), 4.98 (m, 1H), 6.96 (d, 2H), 7.01 (d, 2H), 7.31 (m, 2H), 7.38 (m, 2H), 7.54 (d, 2H), 7.77 (d, 2H). <sup>13</sup>C NMR (101 MHz, CDCl<sub>3</sub>): δ 28.89, 37.31, 47.19, 54.77, 67.31, 78.71, 120.11, 124.52, 125.08, 127.17, 127.87, 129.34, 129.89, 136.72, 139.74, 139.90, 141.42, 142.43, 143.78, 155.01, 155.60, 168.16.

**Synthesis of *N*-(9-Fluorenylmethoxycarbonyl)-*O*-[2,3,4,6-tetra-*O*-acetyl-*D*-galactose-1-(yl)]-tyrosine Pentafluorophenyl Ester (2).** Compound 1 (2.0 g, 3.2 mmol), AgOTf (1.6 g, 6.4 mmol), and molecular sieves (3 Å, 2.5 g) were placed in a predried flask covered with aluminum foil. After evacuation (0.1 Torr), the flask was filled with argon and dry CH<sub>2</sub>Cl<sub>2</sub> (40 mL) was used to suspend the reagents. The suspension was cooled

to -10 °C and a solution of the acetyl bromogalactose (1.1 g, 2.6 mmol) in dry CH<sub>2</sub>Cl<sub>2</sub> (35 mL) was added. After 120 min at -10 °C, the suspension was neutralized with DIPEA (1 mL, 5.74 mmol) followed by filtration through Celite. The filtrate was concentrated to dryness and the residue was purified by column chromatography (silica gel, CH<sub>2</sub>Cl<sub>2</sub>: MeOH 95:5, R<sub>f</sub> 0.32) to yield a white solid. Yield: 70%. <sup>1</sup>H NMR (400 MHz, CDCl<sub>3</sub>): δ 1.98 (s, 3H), 2.00 (s, 6H), 2.10 (s, 3H), 3.21 (m, 2H), 4.00 (m, 1H), 4.11 (m, 2H), 4.21 (m, 1H), 4.44 (m, 2H), 4.98 (m, 1H), 5.09 (m, 1H), 5.30 (m, 1H), 5.40 (m, 1H), 5.51 (m, 1H), 6.97 (d, 2H), 7.13 (d, 2H), 7.28 (m, 2H), 7.38 (m, 2H), 7.50 (d, 2H), 7.75 (d, 2H), 8.31 (broad, CONH, 1H). <sup>13</sup>C NMR (101 MHz, CDCl<sub>3</sub>): δ 20.66, 20.78, 37.21, 47.19, 54.63, 61.42, 66.79, 67.82, 70.81, 71.68, 78.72, 89.80, 120.45, 124.55, 125.05, 127.17, 127.91, 129.39, 129.82, 136.72, 139.74, 139.90, 141.42, 142.40, 143.75, 155.01, 155.61, 168.16, 169.51, 169.92, 170.09, 170.29; C<sub>44</sub>H<sub>38</sub>NO<sub>14</sub>F<sub>5</sub> ESI-MS (M+H<sup>+</sup>) calcd 900.2, found 900.4.

**Synthesis of 1-[2-Oxo-3-aza-9[*N*-(9-fluorenylmethoxycarbonyl)-*O*-[2,3,4,6-tetra-*O*-acetyl-*D*-galactose-1-(yl)]-tyrosinylamine]nonyl]-1,4,7,10-tetraazacyclododecane-4,7,10-triacetic Acid 1,1(Dimethyl)ethyl Ester (3).** To a

Scheme 2. Synthetic Pathway to Gd-DOTAtyr<sup>a</sup>

<sup>a</sup>(I) DOTAMA(OtBu)<sub>3</sub>C<sub>6</sub>NH<sub>2</sub>, HOBT, CH<sub>2</sub>Cl<sub>2</sub>; (II) piperidine, CH<sub>2</sub>Cl<sub>2</sub>; (III) TFA/CH<sub>2</sub>Cl<sub>2</sub>; (IV) GdCl<sub>3</sub>, H<sub>2</sub>O, pH 7.

solution of DOTAMA(OtBu)<sub>3</sub>C<sub>6</sub>NH<sub>2</sub> (0.75 g, 1.1 mmol) in CH<sub>2</sub>Cl<sub>2</sub> (30 mL) was slowly added 2 (1.0 g, 1.1 mmol) in 30 mL of CH<sub>2</sub>Cl<sub>2</sub>. After 20 min, HOBT (0.042 g, 0.28 mmol) and DIPEA (0.19 mL, 1.1 mmol) were added to the reaction mixture and stirred at 0–5 °C under argon atmosphere for 3 h, then for another 16 h at room temperature. The reaction mixture was washed with 10 mL of water and dried over anhydrous Na<sub>2</sub>SO<sub>4</sub>. The filtrate was evaporated to dryness and the white solid was purified by column chromatography (silica gel, elution gradient: CH<sub>2</sub>Cl<sub>2</sub>/MeOH 95:5 → 9:1 → 8:2) to yield a white solid. Yield: 82%. <sup>1</sup>H NMR (600 MHz, CDCl<sub>3</sub>): δ 1.40 (m, 2H), 1.44 (s, 27 H), 1.50 (m, 2H), 1.60 (m, 2H), 1.85 (m, 2H), 1.98 (s, 3H), 2.02 (s, 6H), 2.10 (s, 3H), 2.70–3.60 (broad, 24H), 3.71 (s, 4H), 4.02 (m, 1H), 4.16 (m, 2H), 4.22 (m, 3H), 4.45 (m, 2H), 4.79 (m, 1H), 5.08 (m, 1H), 5.32 (m, 1H), 5.41 (m, 1H), 5.51 (m, 1H), 6.97 (d, 2H), 7.12 (d, 2H), 7.28 (m, 2H), 7.37 (m, 2H), 7.42 (broad, CONH, 1H), 7.51 (d, 2H), 7.74 (d, 2H), 7.89 (broad, CONH, 1H), 8.21 (broad, CONH, 1H). <sup>13</sup>C NMR (151 MHz, CDCl<sub>3</sub>): δ 20.65, 20.72, 25.91, 26.00, 27.90, 28.45, 28.93, 29.66, 37.31, 38.71, 38.81, 47.21, 53.51, 54.54, 55.62, 55.74, 56.17, 54.69, 61.44, 66.72, 67.86, 70.79, 71.65, 78.86, 79.19, 81.6, 89.81, 120.11, 124.41, 125.23, 127.18, 127.82, 129.94, 130.41, 141.42, 143.74, 154.48, 155.89, 155.92, 168.18, 169.57, 169.91, 170.06, 170.31, 171.42, 172.11, 172.23, 172.45, 176, 22; C<sub>72</sub>H<sub>103</sub>N<sub>7</sub>O<sub>20</sub> ESI-MS (M + H<sup>+</sup>) calcd 1386.7, found 1386.9.

**Synthesis of 1-[2-Oxo-3-aza-9[N-(9-fluorenylmethoxycarbonyl)-O-[2,3,4,6-tetra-O-acetyl-D-galactose-1-(yl)]-tyrosinylamido]nonylaminocarbonylmethyl]-1,4,7,10-tetraazacyclododecane-**

**4,7,10-triacetic Acid (4).** The solution of 3 (1 g, 0.72 mmol) in TFA/CH<sub>2</sub>Cl<sub>2</sub> (1:1, 10 mL) was stirred at 0 °C. After 3 h stirring, the reaction mixture was evaporated and the procedure was repeated twice in order to remove all three tBu moieties. Then, the product was precipitated with excess diethyl ether, isolated by centrifugation, washed thoroughly with diethyl ether, and dried in vacuo. The product was used for the next step without further purification: a pale white solid.

**Synthesis of 1-[2-Oxo-3-aza-9[O-[D-galactos-1-(yl)]-tyrosylamido]nonylaminocarbonylmethyl]-1,4,7,10-tetraazacyclododecane-4,7,10-triacetic Acid (5).** The solution of 4 (1.2 g, 0.99 mmol) and NaOMe (0.27 g, 4.9 mol) in methanol (26 mL) was stirred under argon atmosphere at 0 °C. After 5 h stirring, the solution was acidified to around pH 7 with Dowex cationic resin. The reaction mixture was filtered and the solvent evaporated to yield a white solid. The crude material was dissolved in water, loaded over an Amberchrom CG161 column and eluted with a water–methanol gradient (100:0 to 0:100). After solvent evaporation, product 5 was collected as a white solid (yield 65%). <sup>1</sup>H NMR (600 MHz, D<sub>2</sub>O): δ 1.32, 1.42, 1.66 (m, 8H), 2.98–3.16 (broad, 14H), 3.33–3.82 (broad, 22H), 3.93 (m, 1H), 4.99 (m, 1H), 6.87 (d, 2H), 7.12(d, 2H). <sup>13</sup>C NMR (151 MHz, D<sub>2</sub>O): δ 25.54, 25.68, 27.97, 28.24, 34.54, 38.51, 38.43, 53.93, 56.05, 56.12, 56.49, 56.75, 65.55, 69.11, 69.77, 71.84, 73.36, 100.91, 117.92, 128.81, 130.91, 156.44, 169.227, 170.01, 171.96, 178.12; C<sub>37</sub>H<sub>61</sub>N<sub>7</sub>O<sub>14</sub> ESI-MS for (M+H<sup>+</sup>) calcd 828.9, found 828.7. For (M+2H<sup>2+</sup>) calcd 414.9, found 414.7.

**Synthesis of 1-[2-Oxo-3-aza-9[N-(9-fluorenylmethoxycarbonyl)-O-1,1(dimethyl)ethyl-tyrosinylamine]nonyl]-1,4,7,10-tetraazacyclododecane-4,7,10-triacetic Acid 1,1(Dimethyl)ethyl Ester (7).** To a solution of DOTAMA(OtBu)<sub>3</sub>C<sub>6</sub>NH<sub>2</sub> (0.500 g, 0.74 mmol) in CH<sub>2</sub>Cl<sub>2</sub> (25 mL) was slowly added 1 (0.46 g, 0.74 mmol) in 30 mL of CH<sub>2</sub>Cl<sub>2</sub>. After 20 min, HOBT (0.12 g, 0.75 mmol) and DIPEA (0.12 mL, 0.74 mmol) were added and the mixture was stirred for 6 h at 0–5 °C under inert atmosphere. The reaction mixture was then washed with 7 mL of water and dried over anhydrous Na<sub>2</sub>SO<sub>4</sub>. The filtrate was evaporated to dryness and the residue was purified by column chromatography (silica gel, CH<sub>2</sub>Cl<sub>2</sub>/MeOH 9:1) R<sub>f</sub>: 0.38. Yield: 89%. <sup>1</sup>H NMR (600 MHz, CDCl<sub>3</sub>): δ 1.27 (s, 9H) 1.42 (m, 2H), 1.48 (s, 27 H), 1.49 (m, 2H), 1.62 (m, 2H), 1.87 (t, 2H), 2.07–3.30, 3.40–3.50 (b, 22H), 3.54 (s, 4H), 4.23 (m, 3H), 4.40 (s, 2H), 4.45 (m, 1H), 6.97 (d, 2H), 7.12 (d, 2H), 7.28 (m, 2H), 7.37 (m, 2H), 7.43 (broad, CONH, 1H), 7.51 (d, 2H), 7.74 (d, 2H), 7.91 (broad, CONH, 1H), 8.23 (broad, CONH, 1H). <sup>13</sup>C NMR (151 MHz, CDCl<sub>3</sub>): δ 25.93, 26.01, 28.02, 28.57, 28.88, 28.97, 29.67, 37.41, 38.61, 38.91, 46.67, 47.29, 53.01, 53.24, 54.59, 56.22, 56.57, 58.94, 67.31, 78.76, 120.11, 124.81, 125.13, 127.08, 127.62, 129.98, 130.31, 141.42, 143.84, 155.38, 155.83, 169.42, 172.11, 172.23, 172.45, 174.22; C<sub>62</sub>H<sub>93</sub>N<sub>7</sub>O<sub>11</sub> ESI-MS (M+H<sup>+</sup>) calcd 1112.5, found 1112.7.

**Synthesis of 1-[2-Oxo-3-aza-9[-L-tyrosinylamine]nonyl]-1,4,7,10-tetraazacyclododecane-4,7,10-triacetic Acid (8).** The compound 7 (0.91 g, 0.075 mmol) was dissolved in CH<sub>2</sub>Cl<sub>2</sub> (25 mL) containing 10% of piperidine and stirred under inert atmosphere at 0 °C. After 3 h stirring, the solvent was evaporated. Upon the addition of diethyl ether, a white solid was obtained. The crude solid was washed with ice-cooled ether and dried. To the white solid, a solution of TFA/CH<sub>2</sub>Cl<sub>2</sub> (1:1 v/v) was added in one step and stirred. After 4 h, the reaction mixture was evaporated, and the procedure was repeated twice in order to remove all three tBu moieties. Then, the product was precipitated with excess diethyl ether, isolated by centrifugation, washed thoroughly with diethyl ether, and dried in vacuo. It was then dissolved in H<sub>2</sub>O (4 mL) at pH neutralized by addition of diluted NaOH at 0 °C. The crude product was purified by preparative HPLC-ESI (+)MS by using a Waters Atlantis RPdC18 19/100 column by Method 1 using H<sub>2</sub>O/TFA 0.1% (A) and CH<sub>3</sub>CN/TFA 0.1% (B) as eluents (see the Supporting Information). The pure product was obtained as a white powder (Yield 44%). HPLC: Method 2 (see the Supporting Information), retention time 8.90 min, purity 95%. <sup>1</sup>H NMR (600 MHz, D<sub>2</sub>O): δ 1.39, 1.51, 1.60, 1.85 (m, 8H), 2.70–3.60 (broad, 21H), 3.68 (broad, 6H), 4.23 (m, 4H), 6.76 (d, 2H), 6.98 (d, 2H). <sup>13</sup>C NMR (151 MHz, D<sub>2</sub>O): δ 25.76, 25.92, 28.13, 28.32, 36.34, 38.58, 38.75, 53.82, 46.67, 48.51, 51.11, 53.54, 55.27, 116.00, 126.93, 130.97, 155.32, 168.76, 168.89, 171.24, 171.88; C<sub>31</sub>H<sub>51</sub>N<sub>7</sub>O<sub>9</sub> ESI-MS for (M+H<sup>+</sup>) calcd 666.4, found 666.3. For (M+2H<sup>2+</sup>) calcd 333.9, found 333.7.

**Synthesis of Gd-DOTAtyr-gal (6) and Gd-DOTAtyr (9).** To the solutions of DOTAtyr-gal and DOTAtyr ligands (10 mmol) in water (250 mL), a solution containing GdCl<sub>3</sub> (9 mmol) was added. The solution was slowly neutralized to pH 7 with 2 N NaOH. When the pH was constant, the solution was desalted by Sephadex G10 column. The absence of any free Gd(III) ions was checked through the Orange Xylenol spectrophotometric test.<sup>13</sup> Gd-DOTAtyr-gal: C<sub>37</sub>H<sub>58</sub>GdN<sub>7</sub>O<sub>14</sub> ESI-MS (M+H<sup>+</sup>) calcd 983.14, found 983.12. HPLC: Method 2 (Supporting Information), retention time 4.89 min, purity 92%. Gd-

DOTAtyr: C<sub>31</sub>H<sub>48</sub>GdN<sub>7</sub>O<sub>9</sub> ESI-MS (M+H<sup>+</sup>) calcd 821.3, found 821.2. HPLC: Method 3 (Supporting Information), retention time 7.60 min, purity 96%.

**Relaxometric Characterization.** The longitudinal water proton relaxation rate was measured at 25 °C by using a Stelar Spinmaster (Stelar, Mede, Pavia, Italy) spectrometer operating at 20 MHz, by mean of the standard inversion–recovery technique. The temperature was controlled with a Stelar VTC-91 air-flow heater equipped with a copper constantan thermocouple (uncertainty 0.1 °C). The relaxometric characterization of the field-dependent relaxometry of the paramagnetic Gd(III)-probe solutions was carried out through the acquisition of the NMRD profiles. The proton 1/T<sub>1</sub> NMRD profiles were measured at 25 °C on a fast field-cycling Stelar relaxometer over a continuum of magnetic field strengths from 0.00024 to 0.47 T (corresponding to 0.01–20 MHz proton Larmor frequencies). The relaxometer operates under computer control with an absolute uncertainty in 1/T<sub>1</sub> of ±1%. Additional data points in the range 20–70 MHz were obtained on the Stelar Spinmaster spectrometer. The concentration of the solutions used for the relaxometric characterization was determined according to the relaxometric method reported in the Supporting Information section.

**In Vitro Assessment of Enzyme Activity.** To assess the effect of β-galactosidase enzyme on the r<sub>1</sub> value of Gd-DOTAtyr-gal solution, β-galactosidase isolated from *Escherichia coli* was used. *Escherichia coli* enzyme was reconstituted with 0.1 M sodium phosphate buffer, pH = 7.4 at 25.0 ± 0.1 °C. To assess the effect of tyrosinase enzyme on the r<sub>1</sub> value of Gd-DOTAtyr-gal solution, previously activated by β-galactosidase cleavage, tyrosinase isolated from *Mushroom* was used. *Mushroom* enzyme was reconstituted with 0.1 M sodium phosphate buffer, pH = 7.4 at 25.0 ± 0.1 °C.

**Cell Culture.** B16–F10 melanoma cells (mouse) were obtained from American Type Culture Collection (ATCC, Manassas, USA), while B16–F10LacZ cells were obtained from Riken BRC Cell Bank (Depositor Hamada Hirofumi, Japan). Both cell lines were grown in Dulbecco's modified Eagle's medium (DMEM) containing 10% fetal bovine serum from Lonza (Lonza Sales AG, Verviers, Belgium), 100 U/mL penicillin, and 100 mg/mL streptomycin and maintained at 37 °C under 5% CO<sub>2</sub> conditions. After 3 days of culture, the cells were harvested with trypsin/EDTA, counted with the Trypan-blue exclusion test, and assayed for tyrosinase activity.

**Cellular Tyrosinase Activity Assay.** The specific activity of tyrosinase was determined by UV/vis spectrophotometry on a Hitachi U2800 spectrometer using L-DOPA as the substrate and was assayed on the basis of the method reported by Tomita et al.<sup>14</sup> Ca. 1 × 10<sup>6</sup> B16–F10 and B16–F10LacZ cells were washed with PBS, added to 0.5 mL of a 1 mM L-DOPA solution, sonicated to induce cell lysis, and the absorbance at 475 nm was measured over time by maintaining the temperature of the reaction mixture at 37 °C. An extinction coefficient of 3700 M<sup>-1</sup> cm<sup>-1</sup> was used for the quantification of the dopachrome formation.

**Functional β-Galactosidase in Vitro.** Functional expression of β-galactosidase in cells was measured by staining B16–F10LacZ cell by the β-Gal Staining Kit according to the manufacturer's instructions. Cells were grown in small dishes (6 cm in diameter) and fixed with 2 mL fixation solution at room temperature for 15 min. The dishes were washed twice with phosphate buffer solution, and 2 mL staining solution (1 mg/mL X-gal) was added at room temperature until the cells were

stained blue. Cells were examined on microscope (Olympus IX70 inverted).

**Cell Labeling.** The cells were cultured in 75 cm<sup>2</sup> flasks in a humidified incubator at 37 °C and at CO<sub>2</sub>/air (5:95 v/v). 8 × 10<sup>5</sup> B16–F10 and B16–F10*LacZ* cells were seeded in 6 cm Petri dishes. Twenty-four hours after seeding, the incubation medium was removed. Cells were washed and incubated in a fresh DMEM medium with different concentrations (10–15–20 mM) of GdDOTA<sub>tyr</sub>-gal and GdDOTA<sub>tyr</sub> for 4 h at 37 °C in a CO<sub>2</sub> incubator. After this incubation time, the cells were washed three times with 5 mL ice-cold phosphate-buffered saline (PBS), detached with ethylene diamine tetraacetic acid (EDTA), and, for the T<sub>1</sub> measurement at 1.0 T, collected in 50 μL of PBS, transferred into glass capillaries that were centrifuged at 1500 g for 5 min and placed in an agar phantom.

For the electroporation experiment, (3–4) × 10<sup>6</sup> B16–F10*LacZ* cells were detached from the cell culture flask with a trypsin/EDTA solution and placed in an electroporation cuvette containing increasing concentrations of Gd-DOTA<sub>tyr</sub>-gal in 0.8 mL of PBS. The electroporation was performed using Gene Pulser II electroporation system (Bio-Rad Laboratories, Hercules, CA, USA), applying a single shock at 0.2 V, with 500 or 960 microF capacitance and with a time constant of about 10 ms. Cells were then left in ice for 30 min, washed three times with 10 mL ice-cold PBS, and, for the T<sub>1</sub> measurement at 1.0 T, collected in 50 μL of PBS and transferred into glass capillaries that were placed in an agar phantom. T<sub>1</sub> values were measured on an ASPECT M2 System (Israel) operating at 1 T by using a saturation recovery spin echo sequence (TE = 8.6 ms, 12 variable TR ranging from 40 to 3000 ms, NEX = 4, FOV = 1.7 × 1.7 cm<sup>2</sup>, 1 slice, slice thickness = 1 mm).

**Determination of Intracellular Gd<sup>3+</sup> Concentration.** At the end of incubation experiments, labeled B16–F10 and B16–*LacZ* melanoma cells were sonicated in order to destroy cellular membranes and obtain cell lysates. Then, cell homogenates were mineralized with HCl 37% (50:50) in sealed vials at 120 °C overnight and the intracellular content of Gd(III) determined according to the method reported in Supporting Informations. The protein content was determined from cell lysates by the Bradford method using bovine serum albumin as standard. One milligram of protein corresponds to 6.1 × 10<sup>6</sup> B16–F10*LacZ* and 6.3 × 10<sup>6</sup> B16–F10 cells.

**Adhesion Assay.** B16–F10 and B16–F10*LacZ* cells were detached using 2 mM EDTA in PBS, washed with PBS, counted to final concentration of 5 × 10<sup>5</sup> cells/mL and incubated with Gd-DOTA<sub>tyr</sub>-gal (15 mM) and Gd-DOTA<sub>tyr</sub> (15 mM) for 4 h at 37 °C in DMEM containing 10% FBS. The cells were then immediately seeded in 3.5 cm Petri dishes. After 30 min, 1 h, 2 h, and 3 h of incubation, the medium and the floating cells were carefully removed by aspiration, and the attached layers were washed twice with PBS. The firmly attached cells were then counted using a cell counting chamber (Burker-Turk chamber) for quantification. Cell adhesion curves were generated after counting triplicate Petri dishes.

**Animal Model.** 6- to 10-week-old female C57Bl6 mice (Charles River Laboratories, Calco, Italy) were inoculated subcutaneously in the left flank with 0.2 mL of a single suspension containing approximately 1 × 10<sup>6</sup> B16–F10*LacZ* or B16–F10 melanoma cells, respectively. Mice were constantly treated in accordance with European Community guidelines and Ethical Committee Rules of the University of Torino.

**MR Images Studies in Vivo.** To investigate whether β-galactosidase expressing cells could be noninvasively imaged,

C57Bl6 mice (*n* = 6) bearing subcutaneously grown B16–F10 and B16–F10*LacZ* tumors were injected intratumor with 40 μL of Gd-DOTA<sub>tyr</sub>-gal solution (7.5 mM). MR images were acquired on the Aspect M2 system (Aspect Imaging, Shoam, Israel) operating at 1T equipped with a horizontal bore MRI magnet using a standard T<sub>1</sub> weighted multislice spin echo sequence (TR = 250 ms, TE = 7.0 ms, NEX = 10, FOV = 3.5 cm, 6 slices, slice thickness = 1 mm). Prior to MRI examination, animals were anesthetized by injecting tiletamine/zolepam (Zoletil 100), 20 mg/kg, +xylazine (Rompum), 5 mg/kg.

## RESULTS AND DISCUSSION

**Design and Synthesis of Gd-DOTA<sub>tyr</sub>-gal and Gd-DOTA<sub>tyr</sub>.** Gd-DOTA<sub>tyr</sub>-gal was designed to detect β-galactosidase activity through the conversion into Gd-DOTA<sub>tyr</sub> that, in the presence of tyrosinase, polymerizes to form melanin-like structures that are characterized by relaxivity values higher than those of the molecular Gd-DOTA<sub>tyr</sub>-gal and Gd-DOTA<sub>tyr</sub> complexes. Therefore, Gd-DOTA<sub>tyr</sub>-gal consists of three moieties: (i) the outer galacto-pyranose unit that acts as masking group and hampers the start of the polymerization; (ii) the phenolic functionality that in the presence of tyrosinase quickly oxidizes to yield polymeric derivatives; and (iii) the Gd(III) complex that acts as the MRI reporting unit.

Gd-DOTA<sub>tyr</sub> has been synthesized in order to assess its ability to polymerize in tyrosinase containing buffer or cytosol solutions as well as in intact melanoma cells. The melanin-like polymers display a tendency to precipitate as the molecular weight increases. On one hand, this is a limitation because one can exploit only the relaxation enhancement offered by the smaller oligomers. On the other hand, the formation of a polymer implies that the transformed Gd-complexes do not leave the cell and, moreover, their final insolubilization appears as an advantage in terms of limiting the toxicity of the Gd-containing species.

**Relaxometric Characterization of Gd-DOTA<sub>tyr</sub> and Gd-DOTA<sub>tyr</sub>-gal.** The relaxivity of Gd-DOTA<sub>tyr</sub> and Gd-DOTA<sub>tyr</sub>-gal in water, at 20 MHz and 25 °C, is 5.8 and 7.8 mM<sup>-1</sup> s<sup>-1</sup>, respectively. Their relaxivity profiles in the range of frequencies 0.01–70 MHz (NMRD profiles) have been registered and reported in Figure 1. The relaxivity of Gd-DOTA<sub>gal</sub> is slightly higher than that of Gd-DOTA<sub>tyr</sub> at any magnetic field strength because of the higher molecular weight.

The NMRD profiles have been analyzed in terms of the available theory of paramagnetic relaxation, and the main relaxometric parameters have been determined. The two complexes are characterized by similar values for the electronic relaxation time (τ<sub>so</sub> = 160 ps and 150 ps for Gd-DOTA<sub>tyr</sub>-gal and Gd-DOTA<sub>tyr</sub>) and water exchange lifetime (500 ns), while they differ in their reorientational correlation times that were determined to be 192 ps and 125 ps for Gd-DOTA<sub>tyr</sub>-gal and Gd-DOTA<sub>tyr</sub>, respectively.

The cleavage of the galactosyl-pyranose moiety operated by the β-galactosidase enzyme (2 μM) has been followed over time at 37 °C by measuring the change in the relaxation rate (at 20 MHz and 25 °C) of the solutions of Gd-DOTA<sub>tyr</sub>-gal upon addition of the enzyme in phosphate buffer and in serum (Figure 2).

As shown in Figure 2, the transformation of Gd-DOTA<sub>tyr</sub>-gal into Gd-DOTA<sub>tyr</sub>, witnessed by the observed decrease of relaxivity, occurs quite readily either in phosphate buffer or in serum.

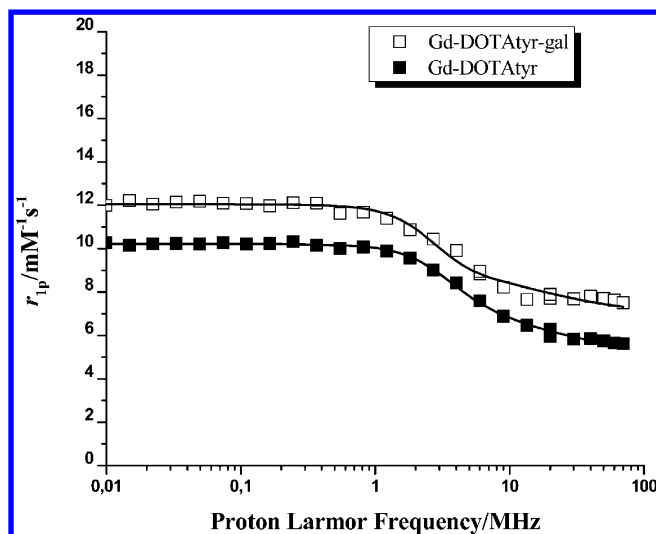


**Figure 1.**  $^1\text{H}$  NMRD profiles of Gd-DOTAtyr-gal ( $\square$ ) and Gd-DOTAtyr ( $\blacksquare$ ) measured at 25 °C and neutral pH. The data refer to the millimolar concentration of the paramagnetic complexes.

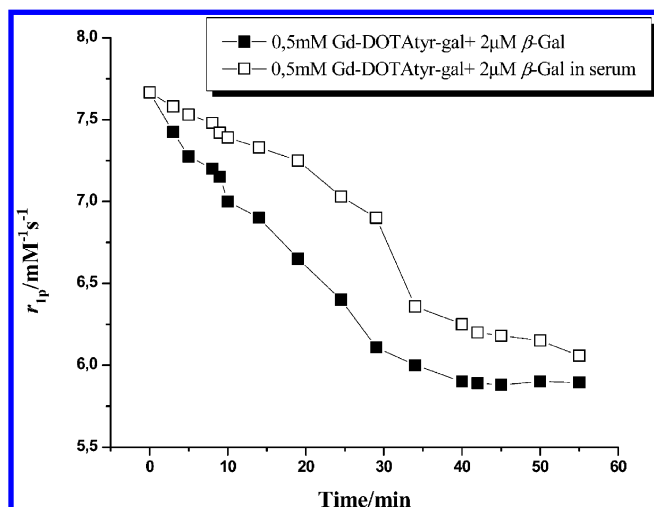


**Figure 2.** Variation of the relaxivity of Gd-DOTAtyr-gal as a consequence of addition of  $\beta$ -galactosidase enzyme in phosphate buffer ( $\blacksquare$ ) and in serum ( $\square$ ). The measurements were carried out at 20 MHz and 25 °C.

Next, the formation of melanin-like polymers from Gd-DOTAtyr in the presence of tyrosinase enzyme has been assessed by either colorimetric and relaxometric measurements. In fact, the formation of melanin-like polymers is characterized by a progressive darkening of the solution (increase of UV absorbance at 475 nm) and by the decrease of the solvent water proton relaxation time (Figure 3).

A similar experiment was also performed on a solution of Gd-DOTAtyr-gal, not activated by  $\beta$ -galactosidase. In this case, no darkening nor any change in the proton relaxation time was observed when the tyrosinase enzyme was added to the solution (Supporting Informations). Having established that Gd-DOTAtyr-gal transforms into Gd-DOTAtyr in the presence of  $\beta$ -galactosidase and Gd-DOTAtyr yields a melanin-like polymer in the presence of tyrosinase, a solution of Gd-DOTAtyr-gal (0.35 mM),  $\beta$ -galactosidase (2  $\mu\text{M}$ ), and tyrosinase (3  $\mu\text{M}$ ) has been prepared and the change in light absorption and proton relaxation times have been measured.

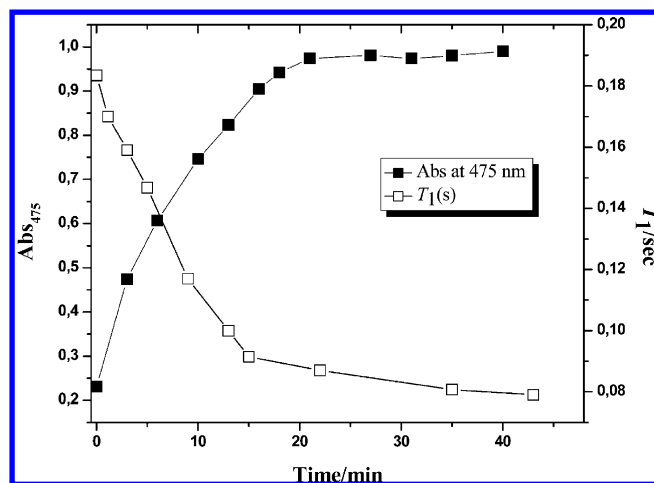


**Figure 3.** Plot of the spectrophotometric ( $\blacksquare$ ) and water proton relaxation time measurements ( $\square$ ) (25 °C, 20 MHz) of a Gd-DOTAtyr (0.35 mM) solution in the presence of tyrosinase enzyme (3  $\mu\text{M}$ ) as a function of time.

The obtained results (Supporting Informations) are very similar to those found for the Gd-DOTAtyr in the presence of tyrosinase. This finding clearly shows that the transformation of Gd-DOTAtyr-gal into Gd-DOTAtyr and then the oligomer formation take place in agreement with what was observed for the separated steps of galactose-pyranose release and melanin formation.

**Relaxometric Analysis of the Activation Process.** An in-depth characterization of the relaxation enhancement for Gd-DOTAtyr-gal solutions upon addition of  $\beta$ -galactosidase and tyrosinase was obtained through the acquisition of the NMRD profiles (Figure 4). As described above, the profile of Gd-

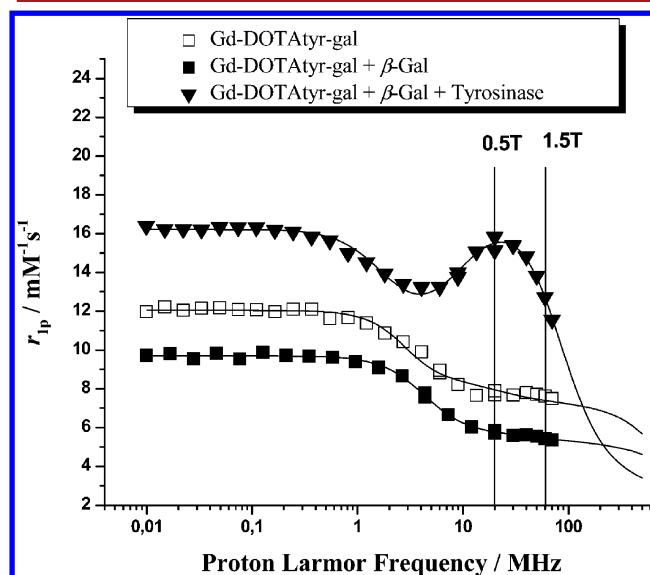


**Figure 4.**  $^1\text{H}$  NMRD profiles of Gd-DOTAtyr-gal ( $\square$ ), Gd-DOTAtyr-gal after the addition of  $\beta$ -Gal ( $\blacksquare$ ), and Gd-DOTAtyr-gal after the addition of  $\beta$ -Gal and tyrosinase ( $\blacktriangledown$ ) registered at 25 °C. The data refer to the millimolar concentration of the paramagnetic complexes. The higher  $r_{1p}$  values observed in the presence of the two enzymes are due to the formation of paramagnetic melanin-like macromolecules.

DOTAtyr-gal complex (open squares) has the classical shape shown by low molecular weight systems. Incubation of Gd-

DOTA<sup>tyr</sup>-gal complex with  $\beta$ -galactosidase at 37 °C for 40 min (red filled squares) led to a decrease of the relaxivity values along the entire range of investigated frequencies. The lower relaxivity is indicative of the formation of the lower molecular weight system ( $\tau_R = 112$  ps) achieved upon the release of the galactose moiety. The obtained profile is in fact almost superimposable with that of the Gd-DOTA<sup>tyr</sup> complex reported in Figure 1. The successive addition of tyrosinase enzyme (3  $\mu$ M) to the remaining complex for 40 min leads to the formation of the oligomerized high relaxivity system (filled triangles -  $\tau_R = 5.6$  ns). Polymerization is the expected reactivity pathway for the phenolic product (obtained by the action of  $\beta$ -galactosidase) in the presence of tyrosinase, in agreement with the previously reported results for Gd-based tyrosinase and myeloperoxidase responsive agents.<sup>8–11</sup>

Investigation into the shapes of the profiles for the polymeric and monomeric Gd-containing systems reveals that there is a strong dependence of the responsiveness of the Gd-probe from the magnetic field strength at which the experiments are carried out. A marked jump in relaxivity is in fact observed in the field range 0.5–1.5 T (working fields of many clinical MR-scanners). At higher field strengths, the differences in relaxivities of the activated and inactivated systems become less marked.

**Enzymatic Activity Assays in B16–F10 and B16–F10LacZ Melanoma Cells.** In order to evaluate more closely the potential of Gd-DOTA<sup>tyr</sup>-gal for cellular applications, tests have been carried out in B16–F10 and B16–F10LacZ murine melanoma cells. Melanoma cells have been used for the enzymatic assays, as these cells possess high tyrosinase activity as witnessed by their natural melanin pigmentation.<sup>15</sup>

Cellular tyrosinase activity was assayed according to the method of Thomita et al. using L-DOPA as substrate and following the conversion of DOPA to DOPochrome via DOPA quinone.<sup>14,16</sup> The increase of absorbance with time reports about the DOPochrome formation and, in turn, on cell tyrosinase activity. Under these conditions, the enzymatic activity of one million B16–F10 and B16–F10LacZ cells has been estimated to be ca. 30 U and 3 U, respectively (by using an extinction coefficient for DOPochrome at 475 nm of 3700 M<sup>-1</sup> cm<sup>-1</sup>). One unit of tyrosinase activity is defined as the amount of enzyme that catalyzes the transformation of 1  $\mu$ mol L-tyrosine/min. The low tyrosinase activity found for B16–F10LacZ fresh homogenates appears to be a frequent phenomenon already reported for other melanoma engineered cells (Figure 5)<sup>14–16</sup> where it has been described as one of the phenotypic variations of cellular differentiation.<sup>18</sup> However when 1  $\times 10^6$  B16–F10LacZ melanoma cells were injected into C57BL/6 mouse, the mouse developed a partially or fully melanotic tumor. This phenomenon, already reported in the literature,<sup>17–19</sup> proved that these cells retained the capacity of producing the pigment, although this capacity appeared not to be well-expressed *in vitro*. Therefore, after being cycled in mice, the B16–F10LacZ cells were again assayed *in vitro* by the method of Thomita et al. using L-DOPA as substrate, and a significant resumption of tyrosinase activity was observed (Figure 5).

To assess the enzymatic activity of  $\beta$ -galactosidase in the cells, B16–F10LacZ cells were stained with  $\beta$ -Gal Staining Kit and examined under optical microscope as shown in Figure 6.

$\beta$ -Gal Staining Kit is based on 5-bromo-4-chloro-3-indolyl- $\beta$ -D-galactopyranoside (X-Gal), a non-inducing chromogenic substrate for  $\beta$ -Gal. The resultant halogenated indigo is a very stable and insoluble dark blue compound (Figure 6).

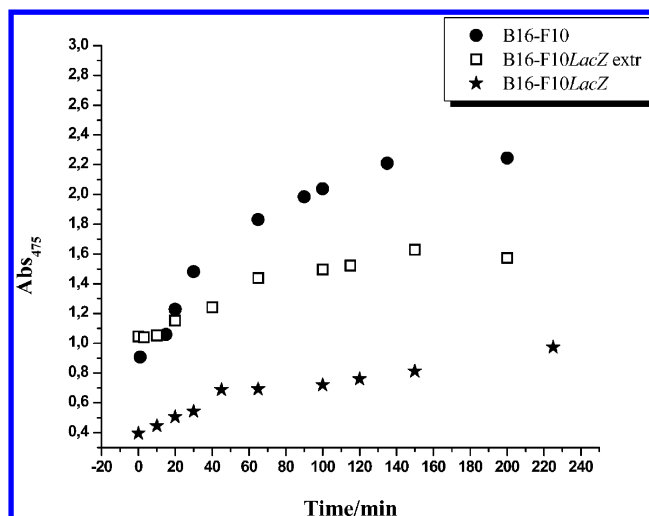


**Figure 5.** Absorbance at 475 nm as a function of time for B16–F10, B16–F10LacZ, and B16–F10LacZ (isolated from injected mice) cells homogenates added to a 0.5 mL of a 1 mM L-DOPA solution.

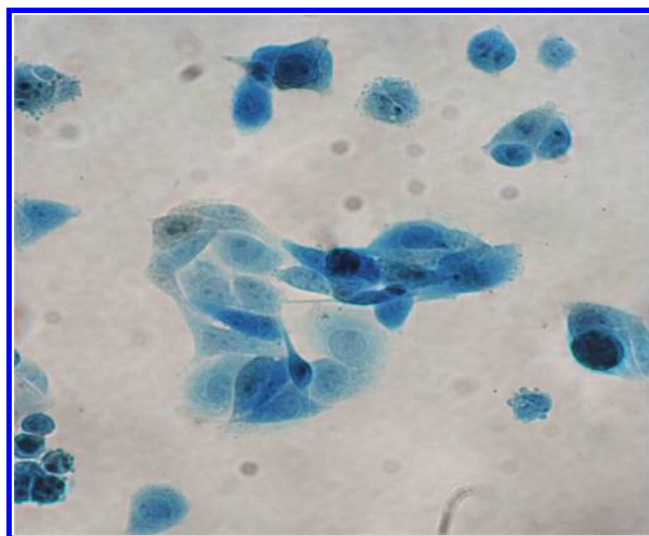


**Figure 6.** B16–F10LacZ cells were stained for  $\beta$ -gal activity by the  $\beta$ -Gal Staining Kit (1 mg/mL X-gal) before examination under the microscope.

**Incubation of Gd-DOTA<sup>tyr</sup>-gal with B16–F10 and B16–F10LacZ Cell Homogenates.** In each experiment, 8  $\times 10^6$  B16F10 or a similar number of B16–F10LacZ cells were added to 100  $\mu$ L of a 1 mM Gd-DOTA<sup>tyr</sup>-gal solution, sonicated to induce cell lysis, and the proton longitudinal relaxation rate at 20 MHz and 25 °C was measured over time while maintaining the temperature of the reaction mixture at 37 °C (Figure 7).

As shown in Figure 7, the relaxivity steadily increases to reach a “plateau” value, after 30 h of incubation. The observed behavior is consistent with the formation of a Gd-incorporated, melanin-like macromolecule. No effect is observed when Gd-DOTA<sup>tyr</sup>-gal is incubated with B16–F10 cells, lacking the  $\beta$ -Gal enzyme.

**Uptake of Gd-DOTA<sup>tyr</sup>-gal and Gd-DOTA<sup>tyr</sup> into B16–F10 and B16–F10LacZ Cells.** Translation of this enzyme-based approach to *in vivo* applications requires that a sufficient amount of Gd-responsive probe is internalized by the cells to be monitored. The uptake efficiency by melanotic B16–



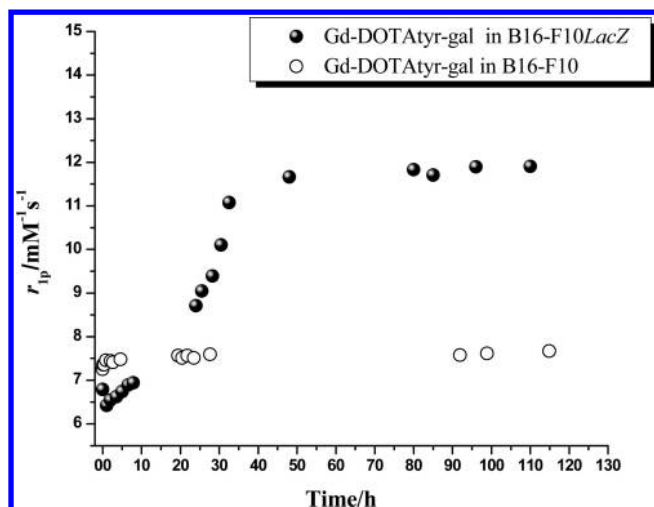


**Figure 7.** Variation of the relaxivity of Gd-DOTAtyr-gal over time in the presence of B16-F10LacZ (●) and B16-F10 (○) cell homogenates. The measurements were carried out at 20 MHz and 25 °C.

F10 and B16-F10LacZ cells was assessed by incubating  $1 \times 10^6$  cells in DMEM medium in the presence of different concentrations (10–15–20 mM) of Gd-DOTAtyr-gal and Gd-DOTAtyr, for 4 h at 37 °C (Figure 8).

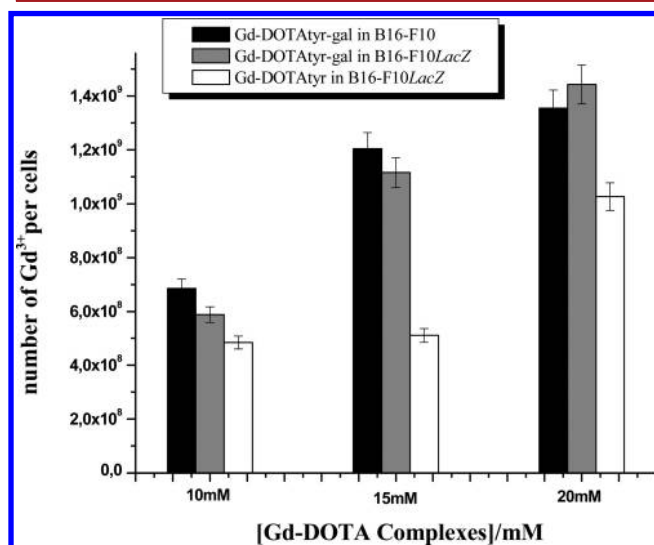


**Figure 8.** Number of  $\text{Gd}^{3+}$  units per cell internalized after incubation of Gd-DOTAtyr-gal in B16-F10 (black) and B16-F10LacZ (gray) cells and Gd-DOTAtyr in B16-F10LacZ cells (white) for 4 h at 37 °C.

The uptake of Gd-DOTAtyr-gal in both  $\beta$ -Gal expressing and parent melanoma cells is significantly higher than that of Gd-DOTAtyr. The higher accumulation efficiency of Gd-DOTAtyr-gal may be accounted for the specific recognition of galectin receptors, which are galactose-specific lectins particularly hyperexpressed on B16-F10 cells.<sup>20,22</sup> Support to the specificity of internalization of Gd-DOTAtyr-gal thanks to the recognition of galectins exposed on cell membrane surfaces has been found in measuring the perturbation of the adhesion of B16-F10 cells to fibronectin of culture dishes. It is in fact known that cell–cell and cell–ECM (extracellular matrix) adhesions are mediated not only by integrin–ligand interactions but also by lectin–saccharide interactions.<sup>20,21</sup>

Recently, El-Boubbou et al.<sup>20</sup> demonstrated that galactose-functionalized magnetic nanoparticles strongly interact with B16-F10 cells, and that this interaction is responsible for a reduction of adherent cells by more than 50%.

Upon incubation of B16-F10LacZ cells with 15 mM Gd-DOTAtyr-gal, we observed a progressive reduction of the amount of adherent cells increasing the incubation time if compared with control cells (Figure 9). In contrast, a very small

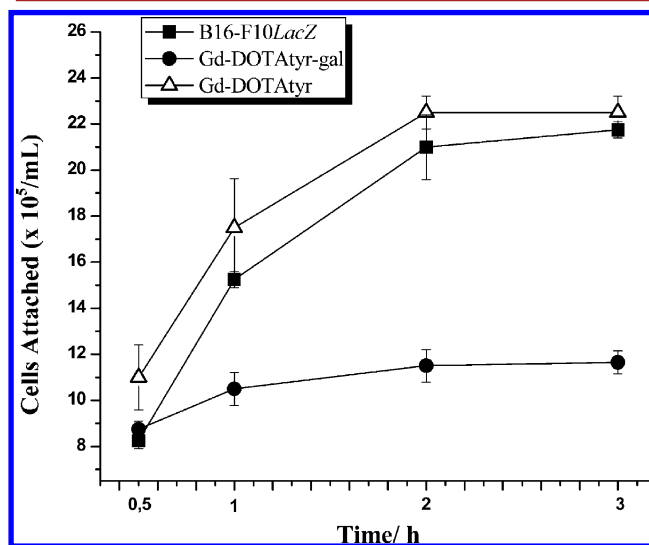


**Figure 9.** Adhesion of mouse melanoma B16-F10LacZ cells to the surface was significantly reduced by incubation with Gd-DOTAtyr-gal (●), while Gd-DOTAtyr ( $\Delta$ ) had no effect on cell adhesion as compared to the cells without any treatment (■).

effect was observed when cells were incubated with Gd-DOTAtyr.

In order to be activated by the cytosolic enzymes, an important issue for the activation of the probe relies on the need to avoid the endosomal compartmentalization of the internalized probe. This issue has been tackled by measuring the variation of observed relaxation rate (at 1T and 25 °C) of the internalized probe as a function of its intracellular concentration (Figure 10). It was recently demonstrated that the occurrence of a linear increase of the observed relaxation rate with the amount of internalized paramagnetic probe is a good reporter of the cytoplasmic localization of the Gd(III)-probe, while a “quenching” effect on the observed relaxation rate is observed in the case of its endosomal entrapment.<sup>23–25</sup> As shown in Figure 10, a linear correlation has been observed, which witnesses that Gd-DOTAtyr-gal, after being internalized by cells, is localized in the cytosol and available for the interaction with  $\beta$ -galactosidase and tyrosinase enzymes. Furthermore, in Figure 10 the relaxation rates of cells labeled via their incubation with Gd-DOTAtyr-gal for 4 h at 37 °C are compared with those obtained for cells in which the same Gd(III)-containing probe has been internalized by electroporation (that invariably leads to a cytoplasmic localization). The two internalization pathways show the same linear growth of observed relaxation rates as a function of the intracellular Gd(III) complex concentration, to support the view that the same cytoplasmic localization is taking place.

**In Vivo MRI Experiments.** To assess the *in vivo* capability of the complex Gd-DOTAtyr-gal to discriminate between

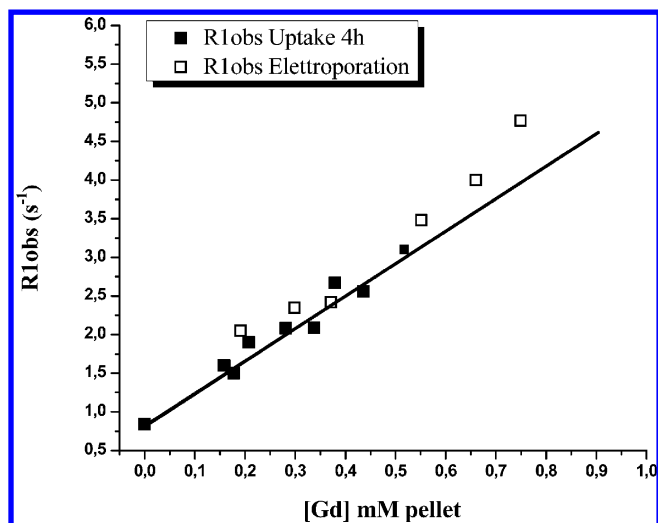


**Figure 10.** Observed longitudinal relaxation rates of B16–F10*LacZ* cellular pellets, measured at 1 T and 25 °C, as a function of Gd<sup>3+</sup> concentration in the cellular pellets from uptake experiments (■) and electroporation experiments (□).

melanoma tumors with and without  $\beta$ -galactosidase gene expression, an MRI study was carried out on two tumor-bearing animal models, namely, (i) C57Bl6 mice grafted with the murine melanoma cell line B16–F10; (ii) C57Bl6 mice grafted with the murine melanoma cell line B16–F10*LacZ*.

The model was obtained by subcutaneous injection of 1 million of B16–F10 or B16-F10*LacZ* cells, on the right limb of six female C57Bl6J mice. At 10–12 days after implantation, a tumor mass of a 2–3 cm width is clearly detectable in each mouse at the site of injection. At this time, animals received

intratumoral injections of the Gd-DOTA<sub>tyr</sub>-gal (40  $\mu$ L of 7.5 mM solution) and  $T_1$  weighted multislice MR images were acquired at 1.0 T.

A strong  $T_1$  contrast was detected in the *LacZ* expressing tumors after 4–5 h from contrast agent injection. At the same detection time, no  $T_1$  contrast was observed in the B16–F10 tumor, which was injected with the same amount of contrast agent (Figure 11a). The observed signal enhancement of the B16–F10*LacZ* tumor was an order of magnitude higher than the one observed for B16–F10 tumor ( $3.5 \pm 1.6$ ) (Figure 11b). The intense enhancement clearly indicates that Gd-DOTA<sub>tyr</sub>-gal is activated by  $\beta$ -galactosidase and tyrosinase enzymes both presented in B16–F10*LacZ* tumor.

## CONCLUSIONS

The  $\beta$ -galactosidase gene *LacZ* is often used as a reporter constructor in eukaryotic transfection experiments due to the proteolytic resistance of the protein product and the easily assayed enzyme activity. In this study, a new Gd(III)-based probe was designed, prepared, and enzymatically tested to be a good  $\beta$ -galactosidase substrate in melanoma B16 homogenate. Upon cleavage by  $\beta$ -galactosidase, the tyrosine residue can interact with the tyrosinase enzyme in B16–F10*LacZ* melanoma cells with subsequent formation of high-relaxivity Gd-DOTA containing oligomers.

A good relaxation enhancement effect was detected. The slow activation of the probe could be due to a relatively low turnover of the enzyme; therefore, higher loading would allow a larger amount of substrate to be converted by the enzyme, thus giving rise to a larger relaxation enhancement effect.

The ability of Gd-DOTA<sub>tyr</sub>-gal to enter B16–F10*LacZ* cells following intratumoral injection has been demonstrated.

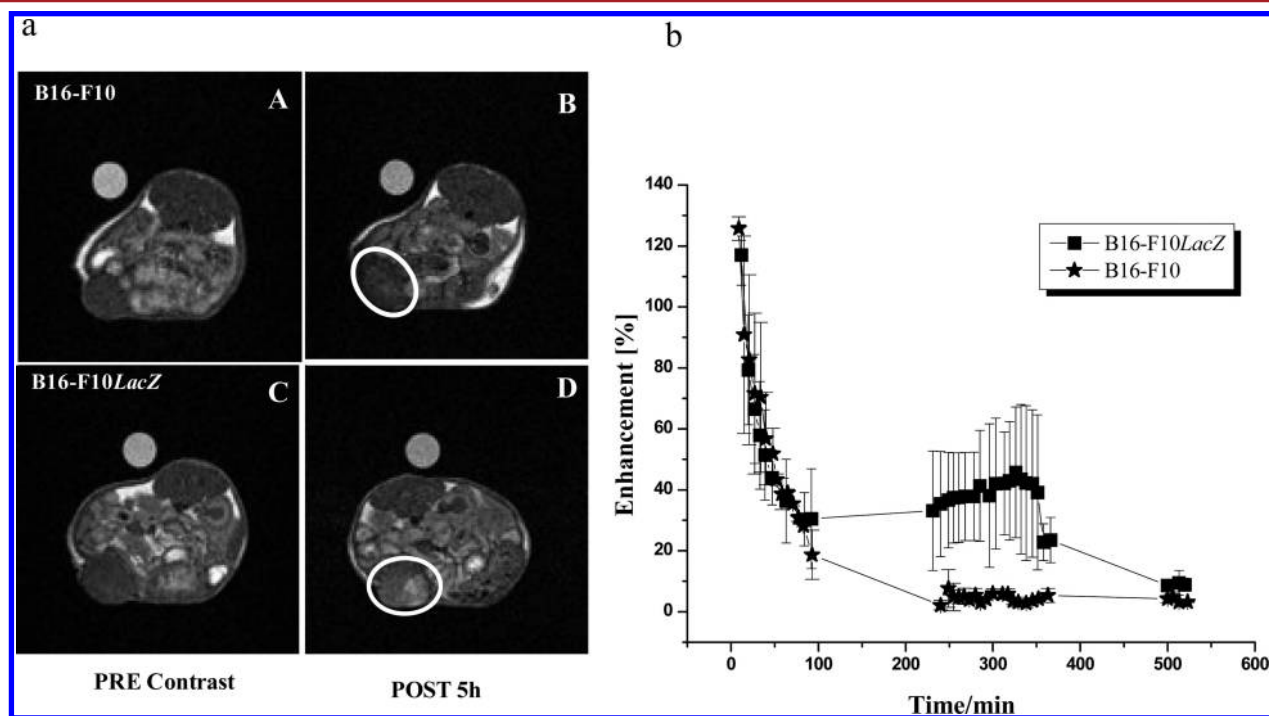


**Figure 11.** (a)  $T_1$ -weighted (TR/TE 250/8.9 ms) MR images of animal model at 1.0 T MR scanner: (A) precontrast image of B16–F10 tumor; (B) at 5 h after intratumoral (IT) injection of 40  $\mu$ L of Gd-DOTA<sub>tyr</sub>-gal (7.5 mM) in B16–F10 tumor; (C) precontrast image of B16–F10*LacZ*; (D) at 5 h after intratumoral (IT) injection of 40  $\mu$ L of Gd-DOTA<sub>tyr</sub>-gal (7.5 mM) in B16–F10*LacZ* tumor; (b) time–signal enhancement change of the B16–F10 and B16–F10*LacZ* tumor after intratumoral (IT) injection of 40  $\mu$ L of Gd-DOTA<sub>tyr</sub>-gal (7.5 mM).

Besides melanoma cells, Gd-DOTATyr-gal would be a good gene reporter for any doubly transfected ( $\beta$ -Gal and Tyr) cells. Finally, the importance of working at low magnetic field strength has been shown when the determinant of the relaxation enhancement is represented by the molecular reorientational time.

## ■ ASSOCIATED CONTENT

### Supporting Information

Control enzymatic activity assays on Gd-DOTATyr-gal and HPLC methods used for the purification of intermediates and final products. This material is available free of charge via the Internet at <http://pubs.acs.org>.

## ■ AUTHOR INFORMATION

### Corresponding Author

\*Fax: +39 0116706487. Tel: +39 0116706451. E-mail: [silvio.aime@unito.it](mailto:silvio.aime@unito.it).

## ■ ACKNOWLEDGMENTS

Economic and scientific support from, EC-FP6-project ENCITE (European Network for "Cell Imaging and Tracking Expertise" 201842), EU-COST D38 Action, Regione Piemonte (PIIMDMT and Nano-IGT projects) is gratefully acknowledged.

## ■ REFERENCES

- (1) Daunert, S., Barrett, G., Feliciano, J. S., Shetty, R. S., Shrestha, S., and Smith-Spencer, W. (2000) Genetically engineered whale-cell sensing systems: Coupling biological recognition with reporter genes. *Chem. Rev.* 100, 2705–2738.
- (2) Cui, W. N., Liu, L., Kodibagkar, V. D., and Mason, R. P. (2010) S-Gal (R), a Novel ( $^1$ H) MRI Reporter for beta-Galactosidase. *Magn. Reson. Med.* 64, 65–71.
- (3) Moats, R. A., Fraser, S. E., and Meade, T. J. (1997) A "smart" magnetic resonance imaging agent that reports on specific enzymatic activity. *Angew. Chem., Int. Ed. Engl.* 36, 725–728.
- (4) Louie, A., Huber, M. M., Ahrens, E. T., Rothbacher, U., Moats, R., Jacobs, R. E., Fraser, S. E., and Meade, T. J. (2000) In vivo visualization of gene expression using magnetic resonance imaging. *Nat. Biotechnol.* 18, 321–325.
- (5) Hanaoka, K., Kikuchi, K., Terai, T., Komatsu, T., and Nagano, T. (2008) A Gd $^{3+}$ -based magnetic resonance imaging contrast agent sensitive to beta-galactosidase activity utilizing a receptor-induced magnetization enhancement (RIME) phenomenon. *Chem.—Eur. J.* 14, 987–995.
- (6) Chang, Y. T., Cheng, C. M., Su, Y. Z., Lee, W. T., Hsu, J. S., Liu, G. C., Cheng, T. L., and Wang, Y.-M. (2007) Synthesis and characterization of a new bioactivated paramagnetic gadolinium(III) complex [Gd(DOTA-FPG)(H $_2$ O)] for tracing gene expression. *Bioconjugate Chem.* 18, 1716–1727.
- (7) Keliris, A., Ziegler, T., Mishra, R., Pohmann, R., Sauer, M. G., Ugurbil, K., and Engelmann, J. (2011) Synthesis and characterization of a cell-permeable bimodal contrast agent targeting beta-galactosidase. *Bioorg. Med. Chem.* 19, 2529–2540.
- (8) Chen, J. W., Pham, W., Weissleder, R., and Bogdanov, A. A. (2004) Human myeloperoxidase: A potential target for molecular MR imaging in atherosclerosis. *Magn. Reson. Med.* 52, 1021–1028.
- (9) Querol, M., Chen, J. W., and Bogdanov, A. A. (2006) A paramagnetic contrast agent with myeloperoxidase-sensing properties. *Org. Biomol. Chem.* 4, 1887–1895.
- (10) Chen, J. W., Querol, M., Bogdanov, A. A., and Weissleder, R. (2006) Imaging of myeloperoxidase in mice by using novel amplifiable paramagnetic substrates. *Radiology* 2, 473–481.

(11) Querol, M., Bennett, D. G., Sotak, C., Kang, H. W., and Bogdanov, A. A. (2007) A paramagnetic contrast agent for detecting tyrosinase activity. *ChemBioChem* 8, 1637–1641.

(12) Barge, A., Tei, L., Upadhyaya, D., Fedeli, F., Beltrami, L., Stefania, R., Aime, S., and Cravotto, G. (2008) Bifunctional ligands based on the DOTA-monoamide cage. *Org. Biomol. Chem.* 6, 1176–1184.

(13) Barge, A., Cravotto, G., Gianolio, E., and Fedeli, F. (2006) How to determine free Gd and free ligand in solution of Gd chelates. A technical note. *Contrast Media Mol. Imaging* 1, 184–188.

(14) Tomita, Y., Maeda, K., and Tagami, H. (1992) Melanocyte stimulating properties of arachidonic acid metabolites – possible role in post-inflammatory pigmentation. *Pigm. Cell Res.* 5, 357–361.

(15) Petrescu, S. M., Petrescu, A. J., Titu, H. N., Dwek, R. A., and Platt, F. M. (1997) Inhibition of N-glycan processing in B16 melanoma cells results in inactivation of tyrosinase but does not prevent its transport to the melanosome. *J. Biol. Chem.* 272, 15796–15803.

(16) Hearing, V. J., and Ekel, T. M. (1976) Mammalian tyrosinase. A comparison of tyrosine hydroxylation and melanin formation. *Biochem. J.* 157, 549–557.

(17) Silagi, S. (1969) Control of pigment production in mouse melanoma cells in vitro. *J. Cell Biol.* 43, 263–274.

(18) Hiroshi, O., Eiko, F., Ichi, N., and Tsutomu, K. (1982) Induction of pigmentation by continuous X-irradiation of amelanotic tumors of B16-XI mouse melanoma and induced change in chromosomes of amelanotic cells. *Cell. Pathol.* 41, 267–276.

(19) Nishii, R., Kawai, K., Garcia Flores, L. II, Kataoka, H., Jinnouchi, S., Nagamachi, S., Arano, Y., and Tamura, S. (2003) A novel radiopharmaceutical for detection of malignant melanoma, based on melanin formation: 3-iodo-4-hydroxyphenyl-L-cysteine. *Nucl. Med. Commun.* 24, 575–582.

(20) El-Boubbou, K., Zhu, D. C., Vasileiou, C., Borhan, B., Prospero, D., Li, W., and Huang, X. (2010) Magnetic glyco-nanoparticles: a tool to detect, differentiate, and unlock the glyco-codes of cancer via magnetic resonance imaging. *J. Am. Chem. Soc.* 132, 4490–4499.

(21) Kim, E. Y. L., Gronewold, C., Chatterjee, A., von der Lieth, C. W., Kleim, C., Schmauser, B., Wiessler, M., and Frei, E. (2005) Oligosaccharide mimics containing galactose and fucose specifically label tumour cell surfaces and inhibit cell adhesion to fibronectin. *ChemBioChem* 6, 422–431.

(22) Oguchi, H., Toyokuni, T., Dean, B., Ito, H., Otsuji, E., Jones, V. L., Sadozai, K. K., and Hakomori, S. (1990) Effect of lactose derivatives on metastatic potential of B16 Melanoma cell. *Cancer Commun.* 2, 311–316.

(23) Terreno, E., Geninatti Crich, S., Belfiore, S., Biancone, L., Cabella, C., Esposito, G., Manazza, A. D., and Aime, S. (2006) Effect of the intracellular localization of a Gd-based imaging probe on the relaxation enhancement of water protons. *Magn. Reson. Med.* 55, 491–497.

(24) Strijkers, G. J., Hak, S., Kok, M. B., Springer, C. S., and Nicolay, K. (2009) Cellular compartmentalization of internalized paramagnetic liposomes strongly influences both T(1) and T(2) relaxivity. *Magn. Reson. Med.* 61, 1049–1058.

(25) Gianolio, E., Arena, F., Strijkers, G. J., Nicolay, K., Högset, A., and Aime, S. (2011) Photochemical activation of endosomal escape of MRI-Gd-agents in tumor cells. *Magn. Reson. Med.* 65, 212–219.